6*β*-Propynyl-Substituted Steroids: Mechanism-Based Enzyme-Activated Irreversible Inhibitors of Aromatase

Abraham Akkani,[†] Germana Paterlini,[†] William B. Gleason,[†,‡] William H. Ojala,[‡] and Yusuf J. Abul-Hajj*[,†]

Department of Medicinal Chemistry and Biomedical Engineering Center and Department of Laboratory Medicine and Pathology, University of Minnesota, Minneapolis, Minnesota 55455

Received May 15, 1997[⊗]

The synthesis and aromatase inhibitory profile of 6α- and 6*β*-propargyl androstenedione and estrenedione are described. The targeted compounds **1** and **2** were prepared by addition of the propargyl Gringard to the 5α,6α-epoxy bisketal **6** or the 5α,6α-epoxy diacetate **7** followed by dehydration of the 6*β*-propargyl 5α-hydroxy diones **10** and **11** using thionyl chloride. Treatment of the 6*β*-propargyl analogs **1** and **2** with hydrochloric acid gave the corresponding 6α-propargyl isomers **3** and **4**. Inhibitory activity of the synthesized compounds was assessed using a human placental microsomal preparation as the enzyme source and [1*β*-^{3}H]-4-androstenedione as substrate. Under initial velocity assay conditions of low product formation, the inhibitors demonstrated potent inhibition of aromatase, with apparent K_is ranging from 10 to 66 nM, with the K_m for androstenedione being 55 nM. 6α-Propargylandrost-4-ene-3,17-dione and 6α-propargylestr-4-ene-3,17-dione were found to be potent competitive inhibitors of aromatase (K_i 37 and 66 nM, respectively). On the other hand the 6*β*-propargylandrost-4-ene-3,17-dione (6*β*-PAD) and 6*β*-propargylestr-4-ene-3,17-dione (6*β*-PED) were found to bind to aromatase with an apparent K_i of 10 and 48 nM, respectively, as well as cause rapid time-dependent, first-order inactivation of aromatase in the presence of NADPH, whereas no inactivation was observed in the absence of NADPH. Substrate protects the enzyme from inactivation, but *β*-mercaptoethanol does not, suggesting that the 6*β*-propargyl analogs 6*β*-PAD and 6*β*-PED are mechanism-based inactivators of aromatase. Energy-minimization calculations and molecular modeling studies indicate three global minima for each of the 6*β*-propargyl analogs in which one of the conformers is proposed to be responsible for the inactivation of aromatase.

Introduction

Aromatase is a cytochrome P450 dependent enzyme that catalyzes the aromatization of androgens to estrogens by three sequential oxidations. The first two oxidative steps are thought to be typical cytochrome P450 hydroxylations while the third step is believed to involve attack of a ferric peroxy species on the aldehyde group of the 19-oxo intemediate as shown in Figure 2.[1,2]

Present knowledge of the mechanism of aromatization has led to the successful design and development of a wide variety of aromatase inhibitors.[3−10] The substrate binding pocket appears to show a lack of tolerance of increased steric bulk at positions C1 and C2, which is contrasted by evidence of a hydrophobic pocket in the region of C4, C6, and C7.[11−14] The orientation of the heme group relative to androstenedione and testosterone has been inferred from the sites of oxidation of the C19 methyl, and from aromatase inhibitors that interact directly with the heme group.[9,15] Although many of these studies provided valuable information on the nature of the interaction of these compounds with aromatase, the lack of knowledge of the enzyme's three-dimentional structure hindered the design of new aromatase inhibitors. Recent site-directed mutagenesis and molecular modeling studies[15−19] of human placental cytochrome $P450_{arom}$, based on sequence alignments

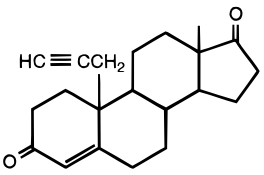

5

Figure 1.

with cytochrome $P450_{cam}$, predicted that the heme iron is positioned in such a way that the distance of the heme iron to atoms C1 and C19 of androstenedione are about 4.9 Å, and the angle between the heme and the steroid A-ring mean planes is about 45°.

Understanding structure−activity relationship in aromatase is of interest not only because of the novelty of the complex series of reactions involved in the aromatization reaction but also because of the importance of developing more potent inhibitors of this enzyme for use in the treatment of breast cancer and other estrogen-related diseases.[20] To further expand on our earlier studies and to explore the nature of interactions of steroidal aromatase inhibitors with the active site of aromatase, we synthesized 6-alkynyl-4-androstenediones and 6-alkynyl-4-estrenediones and evaluated their aromatase inhibitory activity as well as their activity as time-dependent inactivators of aromatase.

Results and Discussion

The synthesis of the intermediates **6** and **7** were carried out as described previously.[21,22] The synthesis

* Corresponding author: Yusuf J. Abul-Hajj, College of Pharmacy, University of Minnesota, Minneapolis, MN 55455.
[†] Department of Medicinal Chemistry.
[‡] Biomedical Engineering Center and Department of Laboratory Medicine and Pathology.
[⊗] Abstract published in *Advance ACS Abstracts,* September 1, 1997.

S0022-2623(97)00325-7 CCC: $14.00

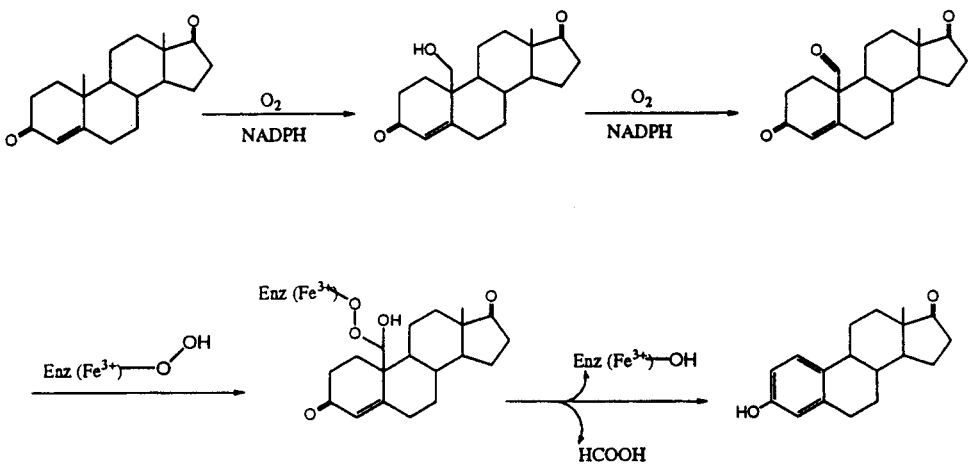

Figure 2. Mechanism of aromatization of androstenedione.

Scheme 1[a]

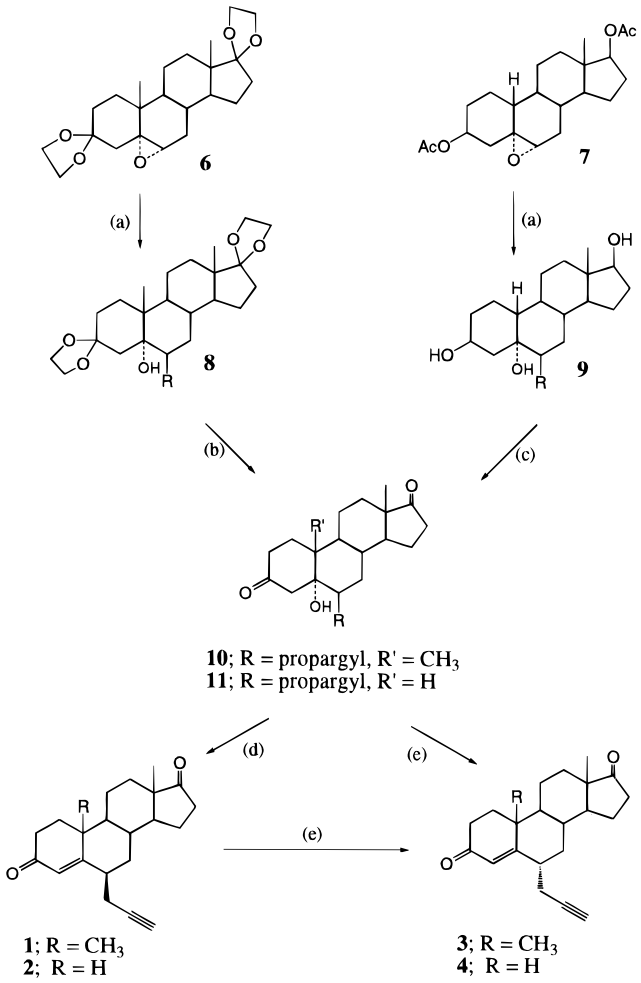

[a] Synthesis of 6β-PAD (**1**), 6β-PED (**2**), 6α-PAD (**3**), and 6α-PED (**4**): (a) RMgBr, THF, rt; (b) TsOH, acetone, rt; (c) CrO_3, acetone, 4 °C; (d) $SOCl_2$, pyridine, 4 °C; (e) HCl, $CHCl_3$, rt.

of the target compounds (6β-PAD, **1**; 6β-PED, **2**; 6α-PAD, **3**; and 6α-PED, **4**), starting from **6** and **7**, is depicted in Scheme 1. Treatment of the 5α,6α-epoxy bisketal **6** with propargylmagnesium bromide gave compound **8** in 70% overall yield. Deprotection of hydroxy ketal **8** with either TsOH or perchloric acid (0.1 M) gave the corresponding 5α-hydroxy dione **10** in quantitative yield, which upon treatment with thionyl chloride gave the final product **1** in 60% yield. The 6α-propargyl analog **3** was obtained in over 85% yield by treatment of either the hydroxy dione **10** or compound **1** under acidic conditions. The synthesis of the 6-alkynylestrenediones **2** and **4** was carried out starting with compound **7**. Addition of the propargylmagnesium bromide to **7** followed by Jones oxidation gave the 5α-hydroxy dione **11**. Dehydration and isomerization of **11** was carried out as described above for the formation of the androstenedione analogs to give high yieds of compounds **2** and **4**.

Table 1. Comparison of Physical Characteristics of 6-Propynyl-4-androstenedione

	6β-PAD (**1**)	6α-PAD (**3**)	Terasawa's compd[a]
mp, °C	159−160	114−116	116−118
IR(KBr), cm^{-1}	3245, 2120	3240, 2150	3300, 1733
	1734, 1662	1740, 1675	1665, 1610[b]
^{1}H-NMR, δ	0.93, 1.26	0.93, 1.22	0.93, 1.22
	2.6−2.8, 5.84	2.3−2.5, 5.81	2.3−2.5, 5.81
MS, m/z (M^+)	324.2	324.2	324

[a] Data obtained from ref 23. [b] IR determined using $CHCl_3$

It is worth noting that a previous report in the patent literature claims the synthesis of compound **1**. However, on the basis of a comparison of the physical characteristics of the compounds reported by Terasawa[23] and those obtained from this investigation (Table 1), it seems that the compound claimed to be the 6β-isomer is actually the 6α-isomer. The ^{1}H-NMR spectra for the 6β- and 6α-propargyl derivatives of androstenedione (**1** and **3**) show some basic differences. The 4-H in the 6α-series is typically a doublet (or a broad singlet), while in the 6β-series the 4-H proton is a sharp singlet (24). The reported peak for the 4-H of Terasawa's propargyl analog is given as a broad singlet. The chemical shifts for the 4-H and C19-CH_3 gave different values for the α- and β- analogs. While the 6β-analog **1** gave values of 5.84 and 1.26 ppm for the 4-H and 19-CH_3, respectively, the 6α analog peaks were observed at 5.81 and 1.22 ppm. Furthermore, the propargyl hydrogen occurs as a multiplet between δ 2.6 and 2.8 for the β-analog, and between 2.3 and 2.5 for the α-analog. In addition, the melting point of our 6α-analog was found to be identical to the compound obtained by Terasawa (Table 1). Conclusive evidence for the structure of **1** was obtained from X-ray crystallographic analysis performed on a single crystal of **1**. Figure 3 is an ORTEP drawing of **1** which clearly shows that the propargyl group in compound **1** is oriented in the β-configuration. Thus,

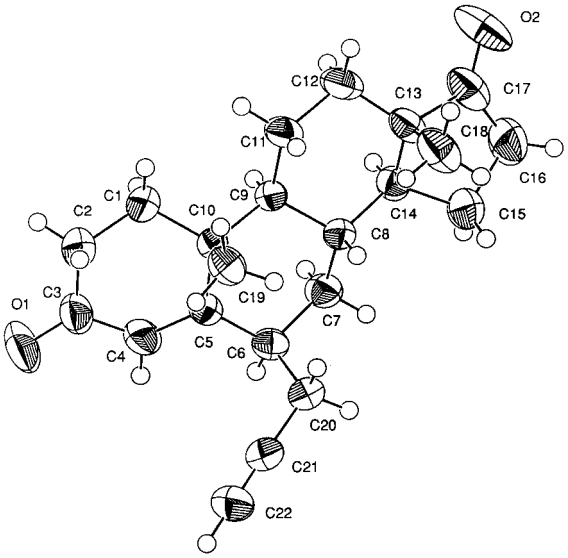

Figure 3. ORTEP diagram of **1** with crystallographic numbering system. Ellipsoids representing the non-hydrogen atoms shown at the 50% probability level.

Table 2. Aromatase Inhibition by 6α- and 6β-Propargyl-Substituted 17-Ketosteroids[a]

compd	IC_{50} (nM)	app K_i (nM)	SE	inhibition
6β-PAD (**1**)	31.0	10	1.1	competitive
6β-PED (**2**)	275	47.6	5.2	competitive
6α-PAD (**3**)	176	37	4.3	competitive
6α-PED (**4**)	187.5	65.8	7.4	competitive
10β-PED (**5**)	56.2	15.2	2.6	competitive
10β-PED (**5**)[b]		68		competitive

[a] Apparent K_i and SE were calculated by a nonlinear regression analysis (ref 31). The apparent K_m for androstenedione was 55 nM (SE = 5 nM). [b] Data obtained from ref 3.

it appears that the step involving the loss of the 5α-OH group from compound **10** plays an important role in the determination of the final configuration of the 6-substituted analogs. The use of acidic conditions as carried out by Terasawa ($CHCl_3$/HCl, room temperature for 16 h) and as shown in our studies leads to the formation of only the 6α-isomers.

6-Substituted steroids **1**, **2**, **3**, and **4** were evaluated *in vitro* by enzyme kinetic studies using human placental microsomes. Aromatase activity in human placental microsomes was assayed by the radiometric method developed by Thompson and Siiteri.[25] This assay quantitates the production of ^3H_2O released from [1β-^{3}H]-4-androstenedione during aromatization. Under initial velocity assay conditions of low product formation, inhibitors were incubated at concentrations ranging from 0 to 500 nM with placental microsomal suspension and androstenedione concentrations ranging from 60 to 500 nM. The 6-substituted propargyl analogs **1**, **2**, **3**, and **4** demonstrated potent inhibition of aromatase with apparent K_i's of 10, 47.6, 37, and 65.8 nM (Table 2). For comparative purposes, we included 10β-propynyl-4-androstenedione (**5**) which has been previously reported as an effective aromatase inhibitor.[3,4] The kinetic mechanism of the 6-propargyl analogs were examined under conditions in which aromatase is rate-limiting. Lineweaver−Burk plots (Figure 4 shows data for 6β-PAD **1**; data for other compounds not shown) for all the compounds exhibited clear cut competitive-type inhibition with respect to androstenedione. Compound **1** was bound with 5 times the affinity of 4-androstenedione,

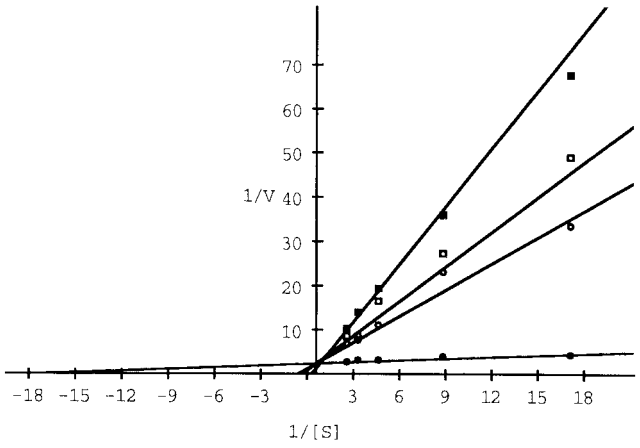

Figure 4. Double-reciprocal plot of aromatase inhibition by 6β-PAD **1**. Varying concentrations of androstenedione were incubated with enzyme at inhibitor concentration of 0.00 (●), 250 (○), 375 (□), and 500 nM (■). Velocity is expressed as (nmol of product/mg of protein)/min and 1/*S* values have units of μM^{-1}. Each point represents the average of two determinations with variations of less that 2% from the mean.

which is somewhat surprising when one considers the increased bulk introduced by the propynyl group. These results are in agreement with those reported earlier[24,26] with other alkyl and aryl 6β-substituted androstenediones.

Each of the newly synthesized propynyl steroids was then tested for their ability to cause time-dependent irreversible inactivation of aromatase in the presence or absence of NADPH cofactor. No time-dependent inactivation was observed when the 6α-analogs **3** and **4** were incubated with aromatase in the presence of NADPH. This is to be expected since the propargyl group in these compounds cannot interact with the heme cofactor. On the other hand, incubation of aromatase, to which an NADPH-generating system was added, for varying time periods with different concentrations of the 6β-analogs **1** and **2** resulted in a time-dependent loss of enzyme activity which followed pseudo-first-order kinetics during the first 12 min of these inactivations (Figure 5). When the enzyme half-life at these different inhibitor concentrations is plotted against the reciprocal of the inhibitor concentration as described by Kitz and Wilson,[27] the apparent kinetic parameters, $T_{1/2}$, $K_{i(inact)}$ and k_{cat} were determined (Table 3). These results show that the rate of inhibition increased linearly with increasing inhibitor concentration, which indicated formation of a dissociable enzyme−inhibitor complex followed by unimolecular activation. Literature k_{cat} and $K_{i(inact)}$ values for **5** (1.11×10^{-3} s^{-1} and 23 nM) compared closely with those obtained in our studies (Table 3). The ratio of k_{cat} to $K_{i(inact)}$ provides a value which has been used to make relative comparisons of the *in vitro* effectiveness of inhibitors. Thus, it would appear from our results that the 6β- and 10β-propargyl analogs **1**, **2,** and **5** behave quite similarly and are shown to be very effective suicide inhibitors of aromatase.

Time-dependent enzyme inactivation required NADPH cofactor (Figure 6), indicating that 6β-PAD must be transformed by aromatase to a reactive intermediate before enzyme inactivation could occur in the active site (Figure 2). Inactivation of aromatase by **1** and **2** was protected by a 2-fold excess of the substrate andros-

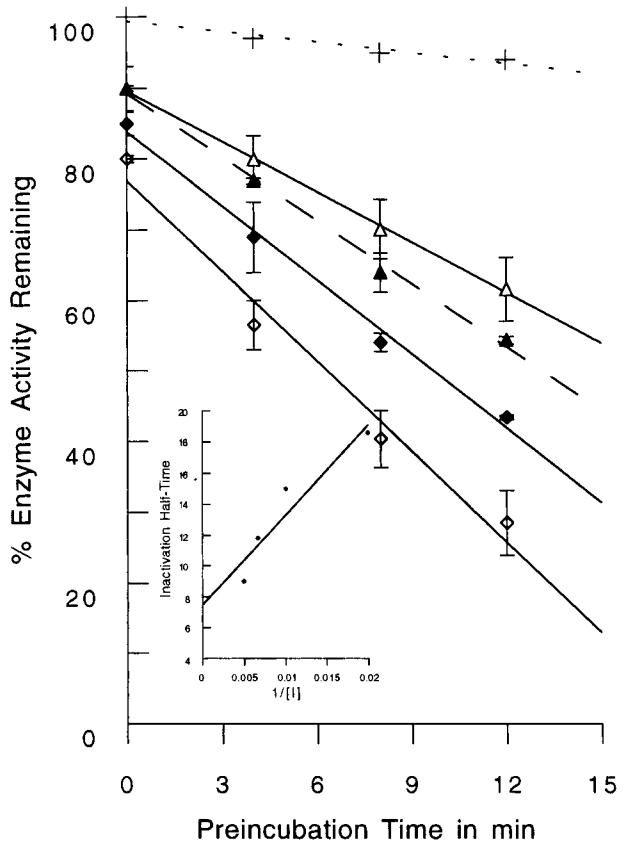

Figure 5. Time-dependent inactivation of human placental aromatase by 6β-PAD (**1**) in the presence of NADPH at inhibitor concentration of 0.00 (+), 50 nM (△), 100 (▲), 150 (◆) and 250 nM (◇). The insert represents a plot of regression analysis of enzyme inactivation rates ($T_{1/2}$) vs reciprocal of inhibitor concentration. The $K_{i(inact)}$ was determined from the intercept of the *X*-axis and the $T_{1/2}$ from the intercept of the *Y*-axis. Each point represents the average of two determinations with less than 6% variation from the mean.

Table 3. Enzyme Kinetic Parameters for 6β-Propargyl 17-Ketosteroids[a]

compd	$T_{1/2}$ (min)	k_{cat} (s^{-1})	app $K_{i(inact)}$ (nM)	k_{cat}/app $K_{i(inact)}$ ($x10^{-6}$)
6β-PAD (**1**)	7.6	1.5×10^{-3}	72.4	21
6β-PED (**2**)	8.9	1.3×10^{-3}	19.8	65
10β-PED (**5**)	8.9	1.4×10^{-3}	59.5	24
10β-PED (**5**)[b]	10.4	1.11×10^{-3}	23	48

[a] Inactivation kinetic values were obtained from plots of the half-time of inactivation vs the reciprocal of the inhibitor concentration (Figure 5). The $T_{1/2}$ values were obtained from the time point at which each half-time reached 50% of its value at zero time. The *y*-intercept of the resulting line (Figure 5 inset) is the half-time of inactivation at infinifte inhibitor ($T_{1/2}$) and the k_{cat} is equal to $0.693/T_{1/2}$. The slope is equal to the product of the *y*-intercept and apparent $K_{i(inact)}$. [b] Data obtained from ref 3.

tenedione, indicating that inactivation by **1** and **2** is active-site directed (Figure 6). The addition of β-mercaptoethanol to the inactivation buffer had no effect on the rate of inactivation, thus ruling out the possibility of inhibition via an affinity-labeling mode by a diffusible alkylating species. Enzyme activity did not return, even after exhaustive dialysis, indicating an irreversible process.

Figure 7 shows a comparison of the rates of inactivation of aromatase by the 6β-propargyl and 10β-propargyl analogs **1**, **2**, and **5** using the same inhibitor concentration of 100 nM. These results as well as the kinetic analysis data presented in Table 3 clearly show that the

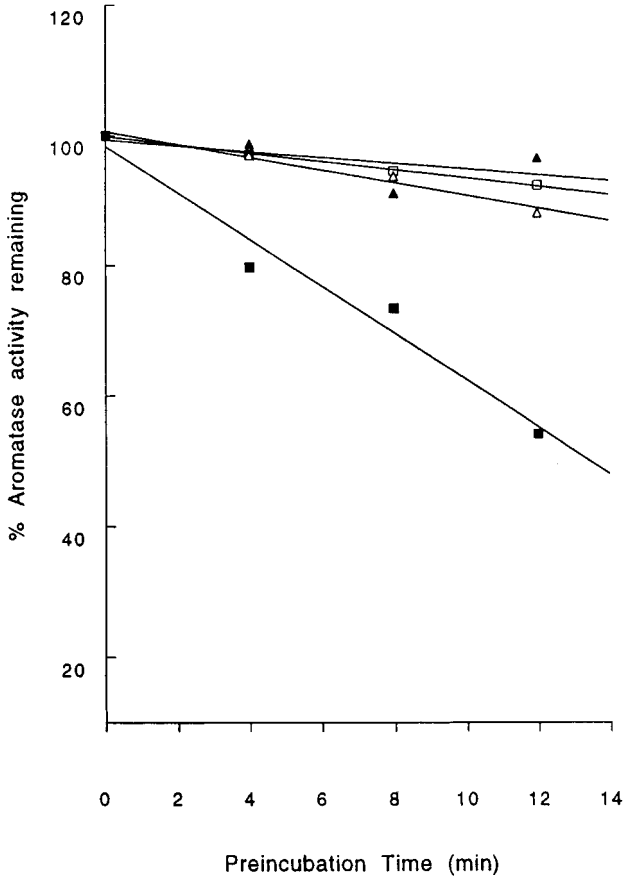

Figure 6. Inactivation of aromatase by 6β-PAD **1** (100 nM) in the presence of NADPH (■); in the absence of NADPH (□); or in the presence of NADPH plus 200 nM androstenedione as a competitive substrate (△). Controls were run simultaneously and contained no inhibitor (▲).

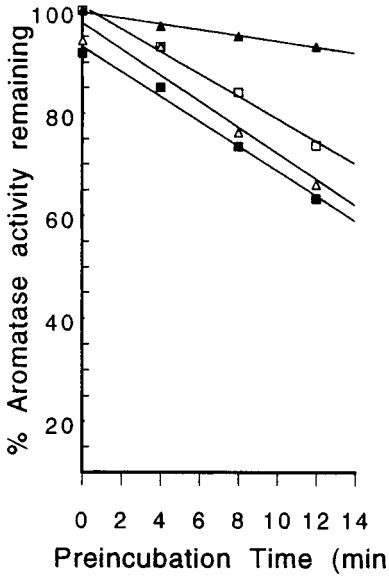

Figure 7. Comparison of inactivation of aromatase by the 6β- and 10β-substituted propargyl 17-ketosteroids. Perincubations were carried out with 100 nM of 6β-PAD **1** (■); 6β-PED **2** (△); or 10β-PED **5** (□). Controls contained no inhibitor (▲).

propargyl analogs behave very similarly in their rate of inactivation and possibly in their overall mechanism of action. Previous studies using 10β-PED (**5**) carried out by Covey *et al.*[3] and Metcalf *et al.*[4] proposed the involvement of either an oxirane species or a Michael acceptor generated by enzyme activation. Whether the

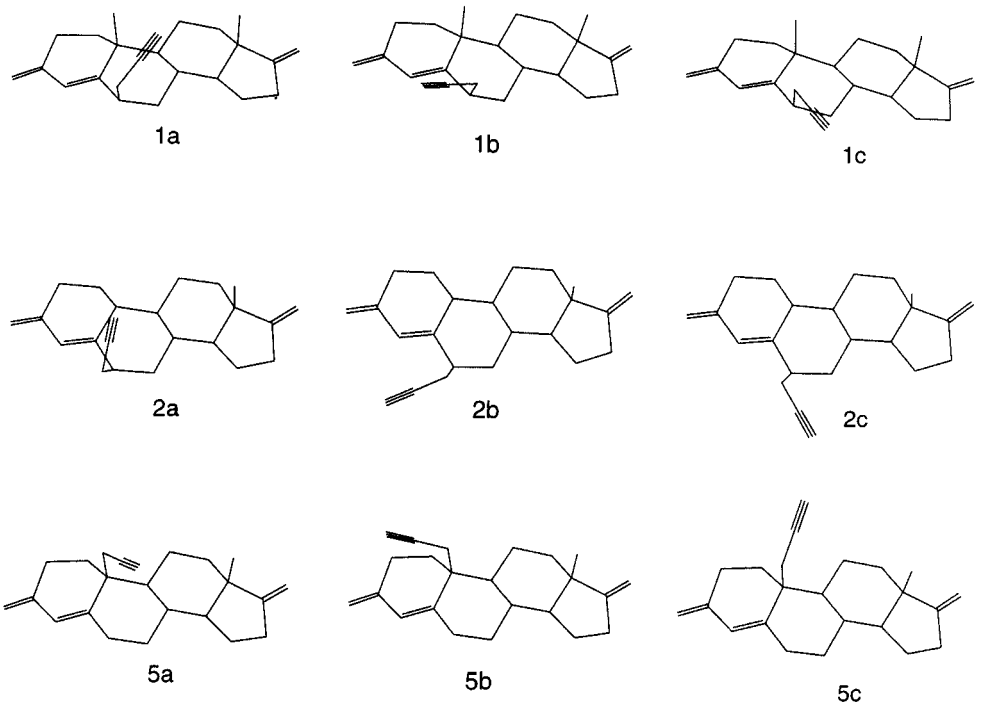

Figure 8. Energy-minimized conformations of 6β-PAD (**1**), 6β-PED (**2**), and 10β-PED (**5**). Coformations of the three local minima for **1**, **2**, and **5** are viewed from the β-side of the steroid nucleus.

formation of the oxirane and/or the Michael acceptor intermediates may be involved in the inactivation of aromatase by 6β-PAD and 6β-PED has yet to be determined.

Previous structure−activity relationship studies by Numazawa and Oshibe[24,26] showed that aromatase has a hydrophobic pocket with a limited accessible volume in the region corresponding to the β-side rather than the α-side of androstenedione. On the basis of these studies and our knowledge from molecular modeling studies on the nature of the interaction of androstenedione with aromatase,[17−19] it was anticipated that introduction of the propargyl moiety at either the 6α- or 6β-positions of androstenedione would produce highly competitive reversible inhibitors of aromatase. To our surprise, however, was the fact that the 6β-propargyl analogs resulted in compounds that are very potent time-dependent inactivators of aromatase. These results could not be reconciled with the predicted orientation of androstenedione with respect to the heme iron.[17,18]

To gain some insight about the conformational differences and similarities between the 6β- and 10β-substituted propargyl steroids, molecular modeling, and energy minimzation analyses were performed on these compounds. Energy-minimization studies on **1**, **2,** and **5** gave three global minima (Figure 8), showing significant differences in the orientation of the propargyl substituent relative to the steroid nucleus. Superposition of conformers **1a**, **2a,** and **5a** (Figure 9) showed that the propargyl group in these analogs occupy approximately the same space and orient above the plane of the steroid ring B, suggesting a common hydrophobic pocket in the active site of aromatase. These results indicate that the inactivation of aromatase by a mechanism-based process by **1**, **2,** and **5** assumes that the heme iron is equidistant from the propargyl group at the 10β- and 6β-positions of estrenedione and androstenedione. However, these observations could not be rationalized on the basis of the results obtained from modeling studies on aromatase in which androstenedione was found to be approximately at a 45° angle from the plane of the heme group.[17,18] Thus, if one assumes the validity of this model of the active site of cytochrome $P450_{arom}$ for the present discussion, then it would be difficult to see how the heme iron oxygen group can activate the acetylenic group in **1** and **2** in which the distances between the heme iron to the acetylenic group in conformers **1a** and **2a** are approximately 8 and 7 Å, respectively. On the other hand, if one holds the heme and heme-binding region fixed, it is proposed that conformers **1a** and **2a** can assume an orientation in which the axis along the C3 to C17 is rotated in such a way that the distance between the heme iron and the 6β-propargyl group in **1a** and **2a** is approximately 4.5 Å, a distance which is compatible with P450 hydroxylations of organic molecules.[28] Since aromatse has not yet been crystallized and the actual orientation of androstendione and the size of the active site binding pocket is not known, it is quite likely that the alternate explanation presented here based on different binding modes of androstenedione and inhibitors is also possible.

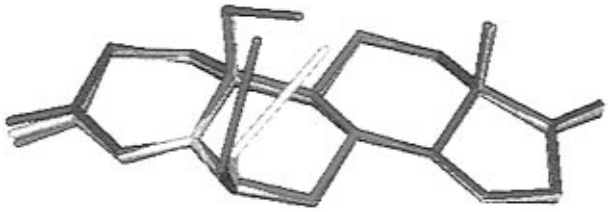

Figure 9. Superposition of conformers **1a** (yellow), **2a** (green), and **5a** (red) showing a common orientation of the propargyl group above ring B.

In conclusion, we have demonstrated that while the 6α-propargyl analogs of 4-androstenedione and 4-estrenedione are effective competitive inhibitors of aromatase, the 6β-propargyl anlogs were found to be very

potent time-dependent inactivators of the enzyme. Inactivation half-times at infinite inhibitor concentration, the k_{app} rates of inactivation (k_{cat}) and the $K_{i(inact)}$'s showed that these compounds behave very similarly to the 10β-propargyl analog, suggesting that the mechanism of inactivation of aromatase by **1**, **2,** and **5** may be quite similar. On the basis of the published mode of interaction of androstenedione with the molecular model of aromatase, we assumed that the 6β-propargyl analogs should not behave as mechanism-based inhibitors. However, the fact that the kinetic data showed that **1** and **2** act as mechanism-based inhibitors led us to propose a different binding mode of interaction of the 6β-propargyl analogs with aromatase. Experiments are underway to investigate the nature of interaction of these compounds with aromatase.

Experimental Section

Melting points were determined on a Fisher Jones melting point apparatus and are uncorrected. Infrared spectra were obtained on a Nicolet 5DXC FT-IR spectrometer. Nuclear magnetic resonance spectra were obtained with a GE 300 MHz spectrometer using TMS as internal standard. Mass spectral data were obtained on a VG 7070 E-HF and a Finnegan MAT 95. TLC was performed on a precoated silica gel plate (silica gel GF; Analtech, Inc., Newark, NJ). Silica gel (200−400 mesh, Aldrich Chemical Co., Milwaukee, WI) was used for all column chromatography. Ultracentrifugation was performed on a Beckman L2-65B ultracentrifuge. Radioactivity was determined using a Beckman LS-100 liquid scintillation counter. Androstenedione was purchased from Steraloids (Wilton, NH). [1β-^{3}H]Androstenedione (24 Ci/mmol) was purchased from New England Nuclear (Boston, MA). All other chemicals were reagent grade and were obtained from Aldrich or Sigma Chemical Co. (St. Louis, MO).

Synthetic Methods. 3,3:17,17-Bis(ethylenedioxy)androstane 5α,6α-Epoxide (6). To a solution of the 3,3:17,17-bis(ethylenedioxy)androst-5-ene (3 g, 8 mmol) in CH_2Cl_2 (50 mL) was added *m*-chloroperbenzoic acid (1.95 g, 11.3 mmol), the mixture was stirred at room temperature for 3 h, diluted with 100 mL of CH_2Cl_2, washed successively with 10% $Na_2S_2O_3$, 5% $NaHCO_3$, brine, and water, and dried over anhydrous Na_2SO_4. The solvent was evaporated in vacuo, and the residue was separated using column chromatography by eluting with hexane/ethyl acetate to afford the 5α,6α-epoxide (1.3 g, 40% yield) and the 5β,6β-epoxide (700 mg, 23%). Crystallization from acetone/hexane afforded the analytical compound: mp 222−223 °C; ^{1}H-NMR ($CDCl_3$) δ 0.79 (s, 3H, 18-CH_3), 1.07 (s, 3H, 19-CH_3), 2.36 (d, 1H, 4-H), 2.81 (d, 1H, 6β-H), 3.8−4.08 (m, OCH_2CH_2O × 2).

6β-Propargyl-3,3:17,17-bis(ethylenedioxy)androstane-5α-ol (8). Grignard reagent was prepared from Mg (0.84 g) and propargyl bromide (4.5 mL) in dry ether with mercuric chloride (50 mg) as initiator under an atmosphere of nitrogen. To the cooled Grignard reagent was added CuCl (50 mg), and the mixture was stirred at room temperature for 5−10 min before the epoxy diketal **6** (600 mg, 1.5 mmol) in dry THF (50 mL) was added. The reaction mixture was stirred for 2-3 h, after which saturated ammonium chloride solution was added and the product was isolated with ethyl acetate. The EtOAc extract was washed with brine and then water, dried over anhydrous Na_2SO_4, and removed in vacuo. The residue obtained was subjected to column chromatography on silica gel, eluting with 25% EtOAc in hexane to give the product **8** in 70% yield: mp 160−162 °C; IR (KBr) 3270 (OH), 3294 C≡CH), and 2100 (C═C) cm^{-1}; ^{1}H-NMR ($CDCl_3$) δ 0.85 (s, 3H, 18-CH_3), 0.94 (s, 3H, 19-CH_3), 3.8−4.0 (m, OCH_2CH_2O × 2).

6β-Propargyl-5α-hydroxyandrostane-3,17-dione (10). The 6β-propargyl bisketal **8** (0.6 mmol) was dissolved in acetone (30 mL), and *p*-TSOH (5 mg) was added. The reaction mixture was stirred at room temperature for 3 h, diluted with EtOAc, successively washed with 5% $NaHCO_3$, brine, and water, and dried over sodium sulfate. The ethyl acetate was removed in vacuo, and the product obtained was purified by column chromatography to yield the pure sample in 90% yield: mp 145−146 °C; IR (KBr) 3475 (C≡CH), 3300 (OH), 2100 (C═C), 1735 and 1715 (C═O) cm^{-1}; ^{1}H-NMR ($CDCl_3$) δ 0.91 (s, 3H, 18-CH_3), 1.21 (s, 3H, 19-CH_3), 3.0 (d, 1H, 4β-H).

6β-Propargyl-4-androstene-3,17-dione (1). The 5α-hyroxy dione **10** (0.3 mmol) was dissolved in dry pyridine (10 mL) and cooled in an ice bath before thionyl chloride was added and the reaction mixture stirred for about 3−5 min. The reaction mixture was poured over ice−water, extracted with ethyl acetate, washed with water, and dried over Na_2SO_4 and the solvent evaporated in vacuo. The residue was subjected to column chromatography (hexane/ethyl acetate) to afford the product which was crystallized from acetone/hexane to yield 60% of the analytical product: mp 159−160 °C; IR (KBr) 3245 (CCH), 2120 (C═C), 1734 and 1662 (C═O) cm^{-1}; ^{1}H-NMR ($CDCl_3$) δ 0.93 (s, 3H, 18-CH_3), 1.26 (s, 3H, 19-CH_3), 2.6−2.8 (m, 1H, C≡CH), 5.84 (s, 1H, 4-H). Anal. ($C_{22}H_{28}O_2$) C, H.

6α-Propargyl-4-androstene-3,17-dione (3). The 6β-propargyl-5α-hydroxy dione (**10**, 300 mg) was dissolved in a 2.5% v/v HCl/$CHCl_3$ mixture (10 mL). The resulting mixture was stirred at room temperature for 2 h, after which it was diluted with water and extracted with CH_2Cl_2 (3 × 50 mL). The organic extracts were combined, washed with $NaHCO_3$ (5%) and water, and dried over Na_2SO_4. The solvent was removed in vacuo, and the product obtained was purified by column chromatography to yield 85% of **3**: mp 114−116 °C; IR (KBr) 3240, 2150, 1740, 1675 cm^{-1}; ^{1}H-NMR ($CDCl_3$) δ 0.93 (s, 3H, 18-CH_3), 1.22 (s, 3H, 19-CH_3), 2.3−2.5 (m, 1H, C≡CH), 5.81 (s, 1H, 4-H). Anal. ($C_{22}H_{28}O_2$) C, H.

3β,17β-Diactoxyestrane-5α,6α-epoxide (7). To a solution of 2 g of the 3β,17β-diacetoxyestr-5-ene in CH_2Cl_2 (70 mL) was added 1.4 g of MCPBA. The mixture was stirred at room temperature for about 2 h, diluted with 50 mL of CH_2Cl_2, and washed successively with 10% $Na_2S_2O_3$, 5% $NaHCO_3$, and water. The organic layer was dried over Na_2SO_4 and evaporated in vacuo to yield a mixture of the α- and β-epoxides which were separated using column chromatography. Elution with hexane/EtOAc (3:1) gave 60% yield of compound **7**: mp 143−145 °C (from methanol); ^{1}H-NMR ($CDCl_3$) δ 0.76 (s, 3H, 18-CH_3), 2.02 (s, 3H, 17-OAc), 2.03 (s, 3H, 3-OAc), 2.98 (d, 1H, 6β-H), 4.56 (t, 1H, 17α-H), 4.95 (m, 1H, 3α-H).

6β-Propargylestrane-3β,5α,17β-triol (9). Preparation of **9** was carried as described for **8**: mp 214−216 °C (from acetone/hexane); ^{1}H-NMR (acetone-d_6) δ 0.74 (s, 3H, 18-CH_3), 3.92 (m, 1H, 3α-H), 3.56 (t, 1H, 17α-H).

6β-Propargyl-5α-hydroxyestrane-3,17-dione (11). The 6β-propargyl triol **9** (0.6 mmol) was dissolved in acetone (30 mL) and cooled down to 4 °C followed by dropwise addition of Jones reagent until the solution turned light brown. The reaction mixture was stirred at 4 °C for approximately 5 min, diluted with water, extracted with EtOAc, successively washed with 5% $NaHCO_3$, brine, and water, and dried over sodium sulfate. The ethyl acetate was evaporated in vacuo, and the product obtained was purified by column chromatography to yield a pure sample of **11** in 90% yield: mp 186−188 °C; ^{1}H-NMR ($CDCl_3$) δ 0.91 (s, 3H, 18-CH_3), 2.65 (d, 1H, 6-H).

6β-Propargyl-4-estrene-3,17-dione (2). The 5α-hyroxy dione **11** was dehydrated as described previously for compound **10**: yield 60%; mp 194−195 °C (from acetone/hexane); ^{1}H-NMR ($CDCl_3$) δ 0.94 (s, 3H, 18-CH_3), 2.73 (m, 1H, C≡CH), 5.94 (s, 1H, 4-H). Anal. ($C_{21}H_{26}O_2$) C, H.

6α-Propargyl-4-estrene-3,17-dione (4). The 6β-propargylestrenedione (**2**) was isomerized to the α-isomer as described for **3**; mp 147−149 °C (from acetone/hexane); ^{1}H-NMR ($CDCl_3$) δ 0.95 (s, 3H, 18-CH_3), 2.65−2.8 (m, 1H, C≡CH), 5.92 (d, 1H, 4-H). Anal. ($C_{21}H_{26}O_2$) C, H.

Biochemical Methods−Enzyme Preparation. Microsomes were obtained from human placentas after normal deliveries and prepared as described previously.[29] Following isolation of the microsomal pellets (washed twice), they were lyophilized and stored at −20 °C. These preparations can be kept for 6 months without loss of activity.

Screening Assay Procedure. The method of Thompson and Siiteri,[25] as modified by Reed and Ohno,[30] was used in our studies. This assay quantitates the production of ^3H_2O

released from [1β-^{3}H]androstenedione during aromatization. All enzymatic studies were performed in 0.1 M phosphate buffer, pH 7.4, at a final incubation volume of 3.0 mL. The incubation mixture contained 5.3 mM glucose 6-phosphate; 0.6 mM NADP; 2 units of glucose-6-phosphate dehydrogenase; various concentrations of inhibitors ranging from 10^{-5} to 10^{-8} M dissolved in ethanol (10 μL/0.5 mL incubation volume); 0.25 μM (0.25 μCi) [1β-^{3}H]androstenedione; 100 μL of propylene glycol; 1.0 mM EDTA; 10 mM phosphate buffer; and 0.25 mg of lyophilized human placental microsomes (33% protein). Incubations were carried out for 15 min at 37 °C and terminated by addition of 5 mL of $CHCl_3$, followed by vortexing for 40 s. After centrifugation at 1500*g* for 5 min, a 0.5 mL aliquot of the aqueous layer was removed and added to 5 mL of scintillation mixture for determination of ^3H_2O production.

Time-Dependent Inactivation Studies. Various concentrations of inhibitors were incubated at 37 °C with placental microsomal protein (0.08−0.1 mg/mL), propylene glycol (100 μL), and NADPH (0.1 mM) in 0.1 M phosphate buffer, pH 7.4, to a total volume of 10 mL. Aliquots (1.0 mL) were removed at various time periods and immediately diluted 10-fold with cold buffer. The remaining enzyme activity was assayed by addition of the microsomal suspension to a solution of [1β-^{3}H]-androstenedione [0.25 μM (0.25 μCi)], propylene glycol (100 μL), NADP (0.6 mM), glucose 6-phosphate (5.3 mM), glucose-6-phosphate dehydrogenase (2 units) in 0.1 M phosphate buffer, pH 7.4, to give a final volume of 3.0 mL, and incubated at 37 °C for 30 min. The incubations were then processed as above.

K_i Assay Procedure. Kinetic studies were carried out under initial velocity conditions. Analysis conditions employed [1β-^{3}H]androstenedione progressively diluted with inert androstenedione (0.005−0.25 μM). Incubations employed 0.025−0.03 mg of microsomal protein in 1.0 mL of 0.1 M phosphate buffer (pH 7.4) at 37 °C in air for 10 min and were processed as described above. Control samples with no inhibitor were incubated simultaneously, and blank samples were incubated for 0 min. Each inhibitor was examined at three concentrations (250, 375, and 500 nM). The enzyme kinetic data were analyzed by regression analysis programs.[31]

Modeling Studies. Modeling studies were conducted using Biosym Software, Insight II 2.3 and Discover 2.9.[32] Calculations made use of atomic charges obtained using a Gaussian 94[33] with a STO-3G basis and of consistent valence forcefield (cvff) parameters supplied with the Biosym package. The molecules were initially energy minimized using 300 steps of the steepest descent algorithm. A systematic search for conformers was then carried out by freely rotating (360° in 10° interval) the propargyl group around the following dihedral angles: C5−C6−C20−C21 for **1** and **2** and C5−C10−C19−C20 for **5**. The resulting conformers were again energy minimized using 300 steepest descent minimization steps. Energy minima were found at −77 (E = 98.1), 65 (96.4), and 168 (E = 94.0) for **1**; −60 (E = 48.9), 72 (E = 49.6), and 180 (E = 48.7) for **2**; −58 (E = 57.0), 70 (E = 55.1), and −175 (E = 55.9) for **5**.

X-ray Crystallography. Colorless crystals of **7** were grown in acetone/hexane. All measurements were made on a Rigaku AFC6S X-ray diffractometer with graphite monochromated Cu Kα radiation (λ = 1.541 78 Å) using the ω-2θ scan mode. The crystal temperature was maintained at 173(1) K by using a Molecular Structure Corporation low-temperature device. Intensities were corrected for Lorentz and polarization effects. Equivalent reflections were merged, and absorption effects were corrected using the ψ scan technique (transmission factors: 0.96−1.00) as described by North et al.[34] The structure was solved by direct methods using SHELXS86[35] and refined and finished using the TEXSAN structure analysis package.[36] All non-hydrogen atoms were refined anisotropically. Hydrogens bonded to carbon atoms were placed in calculated positions (0.95 Å) and were not refined. Hydrogens bonded to heteroatoms were located in difference Fourier maps, and their positional parameters were refined.

Acknowledgment. This work was supported in part from PHS Grant TW 05132 (A.A.) and CA 57615 (Y.J.A.).

Supporting Information Available: The X-ray crystallographic data for compound **1** (22 pages). Ordering information is given on any current masthead page.

References

(1) Oh, S. S.; Robinson, C. H. Mechanism of Human Placental Aromatase: A New Active Site Model. *J. Steroid Biochem. Mol. Biol.* **1993**, *44*, 389−397.
(2) Akhtar, M.; Njar, V. C. O.; Wright, J. N. Mechanistic Studies on Aromatase and Related C-C Bond Cleavage P-450 Enzymes. *J. Steroid Biochem. Mol. Biol.* **1993**, *44*, 375−387.
(3) Covey, D. F.; Hood, W. F.; Parikh. V. D. 10β-Propynyl-substituted Steroids. *J. Biol. Chem.* **1981**, *256*, 1076−1079.
(4) Metcalf, B. W.; Wright, C. L.; Burkhart, J. P.; Johnston, J. O. Substrate-induced Inactivation of Aromatase by Allenic and Acetylinic Steroids. *J. Am. Chem Soc.* **1981**, *103*, 3221−3222.
(5) Abul-Hajj, Y. J., Liu, X.-P.; Hedge, M. Synthesis and Evaluation of Substituted-4-androstene-3,17-dione Derivatives as Aromatase Inhibitors. *J. Steroid Biochem. Mol. Biol.* **1995**, *54*, 111−119.
(6) O'Reilly, J. M.; Williams, N. L.; Duax, W. L.; Brueggemeier, R. W. Synthesis, Structure Elucidation, and Biochemical Evaluation of 7α- and 7β-Arylaliphatic-substituted Androst-4-ene-3,-17-diones as Inhibitors of Aromatase. *J. Med. Chem.* **1995**, *38*, 2842−2850.
(7) Brodie, A. M.; Schwarzel, W. C.; Sheikh, A. A.; Brodie, H. J. The Effect of an Aromatase Inhibitor, 4-Hydroxy-4-androstene-3,-17-dione, on Estrogen Dependent Progress in Reproduction and Breast Cancer. *Endocrinology* **1977**, *100*, 1684−1695.
(8) Bednarski, P. J.; Nelson, S. D. Interactions of Thiol-containing Androgens with Human Placental Aromatase. *J. Med. Chem.* **1989**, *32*, 203−213.
(9) Kellis, J. T.; Childers, W. E.; Robinson, C. H.; Vickery, L. E. Inhibition of Aromatase Cytochrome P-450 by 10-Oxirane and 10-Thiirane Substituted Androgens. *J. Biol. Chem.* **1987**, *262*, 4421−4426.
(10) Osawa, Y.; Osawa, Y.; Coon, M. J. Stereochemistry of the Functional Group Determines the Mechanism of Aromatase Inhibition by 6-Bromoandrostenedione. *Endocrinology* **1987**, *121*, 1010−1016.
(11) Laughton, C. A.; Neidle, S. Inhibition of the P450 Enzymes Aromatase and Lyase. Crystallograhic and Molecular Modeling Studies Suggest Structural Features of Pyridylacetic Acid Derivatives Responsible for Differences in Enzymic Inhibitory Activity. *J. Med. Chem.* **1990**, *33*, 3050−3060.
(12) Brueggemeier, R. W.; Floyd, E. E.; Counsell, R. E. Synthesis and Biochemical Evaluation of Inhibitors of Estrogen Biosynthesis. *J. Med. Chem.* **1978**, *21*, 1007−1011.
(13) Abul-Hajj, Y. J. Synthesis and Evaluation of 4-(Substituted thio)-4-androstenedione Derivatives as Potential Aromatase Inhibitors. *J. Med. Chem.* **1986**, *29*, 582−584.
(14) Liu, X.-P.; Lambert, D. M.; Abul-Hajj, Y. J. Probing the Hydrophobic Pocket of the Active Site of Aromatase with 4-Phenoxy-7α-thiophenyl-4-androstenedione. *J. Med. Chem.* **1995**, *38*, 4135−4138.
(15) Kellis, J. T.; Vickery, L. E. The Active Site of Aromatase Cytochrome P-450. *J. Biol. Chem.* **1987**, *262*, 8840−8844.
(16) Chen, S,; Zhou, D.; Swiderek, K. M.; Kadohama, N.; Osawa, Y.; Hall, P. F. Structure-Function Studies of Human Aromatase. *J. Steroid Biochem. Mol. Biol.* **1993**, *44*, 347−356.
(17) Graham-Lorence, S.; Khalil, M. W.; Lorence, M. C.; Mendelson, C. R.; Simpson, E. R. Structure-Function Relationship of Human Aromatase Cytochrome P-450 Using Molecular Modeling and Site-Directed Mutagenesis. *J. Biol. Chem.* **1991**, *266*, 11939−11946.
(18) Laughton, C. A.; Zvelebil, M. J. J. M.; Neidle, S. A Detailed Molecular Model for Human Aromatase. *J. Steroid Biochem. Mol. Biol.* **1993**, *44*, 399−407.
(19) Graham-Lorence, S.; Amarneh, B.; White, R. E.; Peterson, J. A.; Simpson, E. R. A Three-Dimennsional Model of Aromatase Cytochrome P450. *Protein Sci.* **1995**, *4*, 1065−1080.
(20) Santen, R. J.; Manni, A.; Harvey, H.; Redmond, C. Endocrine Treatment of Breast Cancer. *Endocrine Rev.* **1990**, *2*, 1−45.
(21) Campbell, J. A.; Babcock, J. C.; Hogg, J. A. 6-Methylsteroids in the androstane series. *J. Am. Chem. Soc.* **1958**, *80*, 4714−4721.
(22) Viollotti, R.; Djerassi, C.; Ringold, H. J. Steroids. CXXIII. 19-Nor-6-methylandrostane Derivatives. *J. Am. Chem. Soc.* **1959**, *81*, 4566−4570.
(23) Terasawa, T. Aromatase Inhibition by Steroid Derivatives. Jap. Patent 63-45294, February 26, 1988.
(24) Numazawa, M.; Oshibe, M. 6-Alkyl- and 6-Arylandrost-4-ene-3,17-dione as Aromatase Inhibitors. Synthesis and Structure-Activity Relationships. *J. Med. Chem.* **1994**, *33*, 1312−1319.

(25) Thompson, A. E., Jr.; Siiteri, P. K. The Involvement of Human Placental Microsomal P-450 in Aromatization. *J. Biol. Chem.* **1974**, *249*, 5373−5378.
(26) Numazawa, M.; Oshibe, M. Further Studies on 6-Alkylandrost-4-ene-3,17-dione as Aromatase Inhibitors: Elongation of the 6-Alkyl Chain. *Steroids* **1995**, *60*, 576−581.
(27) Kitz, R.; Wilson, I. B. Esters of methansulfonic acid as irreversible inhibitors of acetycholinesterase. *J. Biol. Chem.* **1962**, *237*, 3245−3249.
(28) Poulos, T. L.; Finzel, B. C.; Howard, A. J. High resolution crystal structure of cytochrome $P450_{cam}$. *J. Mol. Biol.* **1987**, *195*, 687−700.
(29) Ryan, K. J. Biological Aromatization of Steroids. *J. Biol. Chem.* **1959**, *234*, 266−272.
(30) Reed, K. C.; Ohno, S. Kinetic properties of human placental aromatase. *J. Biol. Chem.* **1976**, *251*, 5373−5378.
(31) Cleland, W. W. The statistical analysis of enzyme kinetic data. *Methods Enzymol.* **1979**, *63*, 103−138.
(32) Biosym Technologies, 9685 Scranton Rd., San Diego, CA 92121−2777.
(33) Gaussian Inc., Carnegie Office Park, Pittsburgh, PA 15106.
(34) North, A. C. T.; Phillips, D. C.; Mathews, F. S. A semiempirical method of absorption correction. *Acta Crystallogr. Sect. A* **1968**, *24*, 351−359.
(35) SHELXS 86. Program for the solution of crystal structures, University of Göttingen, Germany, 1985.
(36) TEXSAN-TEXRAY. Structure Analysis Package, Molecular Structure Corporation, The Woodlands, TX, 1985.

JM970325Z